ELSEVIER

Physica A 232 (1996) 713–722

PHYSICA A

Atomic correlations in AlCo decagonal approximant phases

Mike Widom [a,*], Eric Cockayne [b,1]

[a] *Department of Physics, Carnegie-Mellon University, Pittsburgh, PA 15213, USA*
[b] *Laboratoire de Physique des Solides (associé au CNRS), Bâtiment 510, Université Paris Sud, 91405 Orsay Cedex, France*

Abstract

Many distinct phases of aluminum cobalt alloys occur in a narrow composition range near Al_3Co. We compare the distribution functions of these structures with pair potentials calculated for this binary alloy. Both the Al–Co and the Co–Co distributions display strong modulations out to distances of beyond 10 Å, while the Al–Al distributions approach a constant beyond a few Angstroms. Radial distribution function peaks generally fall in the vicinity of pair potential minima. We show how energetically favorable interatomic spacings relate to local atomic arrangements in a cluster known as a pentagonal bipyramid. Filling space with this cluster suggests a possible tiling model for the decagonal phase.

1. Introduction

Aluminum–cobalt alloys form a large number of equilibrium phases with large unit cells near the composition Al_3Co [1,2]. These phases all appear to be approximants to decagonal quasicrystals, which means they contain pseudo-decagonal structural motifs and their diffraction patterns resemble the quasicrystal phase diffraction patterns. Under the assumption that structures with similar diffraction patterns are closely related, the various approximants share a degree of structural similarity with each other and with the (as yet unknown) structure of the metastable Al-Co decagonal as well. Note that the decagonal quasicrystal is a metastable structure among aluminum-cobalt binary alloys, but becomes thermodynamically stable when alloyed with nickel or copper [11].

We can express the total energy of a configuration of atoms as a sum of interactions between clusters of atoms [12,10]. For aluminum-rich intermetallic alloys [3], we believe the dominant structure dependent term in this sum to be the pair potential

* Corresponding author.
[1] Current address: Department of Applied Physics, Yale University, New Haven, CT 06520 USA

PII S0378-4371(96)00179-3

$V_{\alpha\beta}(r)$ between atoms of species α and β spaced by distance r. The pair interaction contribution to the total energy relates directly to the radial distribution functions $g_{\alpha\beta}(r)$ as

$$E = 2\pi\mathcal{V}\sum_{\alpha\beta}\rho_\alpha\rho_\beta\int_0^\infty V_{\alpha\beta}(r)g_{\alpha\beta}(r)r^2dr\,. \tag{1}$$

Here $\rho_{\alpha,\beta}$ are the partial densities and $\mathcal{V}$ the total volume. We compare the radial distribution functions of known structures with each other and with predicted pair potentials to understand the multiplicity of stable phases. Up to 10 Å, radial distribution function peaks match well with pair potential minima. The strongest peaks in $g_{\alpha\beta}$ occur when at least one of the two species is cobalt. The aluminum-aluminum correlations are considerably weaker and shorter-ranged than those involving cobalt.

In addition we present results of Monte Carlo simulations on a hypothetical approximant showing spontaneous formation of structures with similar radial distribution functions (and similar real space structure) and we simulate the thermal fluctuations in the structure. Because our simulation technique places atoms only at discretely spaced "ideal" sites, phonons are prohibited, and the dominant thermal fluctuations in our simulation are the so-called "phason fluctuations".

2. Pair potentials

Pair interactions between ions in metals display long-ranged oscillations associated with the Fermi wavevector. Asymptotically, the potentials fall off as

$$V(r) \sim \frac{\cos(2k_Fr-\delta)}{r^3}\,. \tag{2}$$

These oscillations appear in Fig. 1 showing pair potentials calculated by Phillips et al. [3] for aluminum–cobalt alloys. The Fermi wavevector k_F depends on the electron density, which Phillips et al. take as $0.18076\,\text{Å}^{-3}$, the value for pure FCC aluminum. The binary structures studied here have estimated electron densities close to this value, assigning valence $Z = +3$ for aluminum and $Z = +1.5$ for cobalt.

Rather than recalculate the potentials for each electron density, in the following we perform computer simulations at chemical compositions with the electron density of FCC aluminum. We explain how to rescale axes of experimentally determined structures to match this density. Thus the Fermi wave-vector takes the value for FCC aluminum, $k_F = 1.749\,\text{Å}^{-1}$, and the interaction potentials have minima spaced, asymptotically, by

$$\Delta R = \pi/k_F = 1.796\,\text{Å}\,. \tag{3}$$

The Al–Co interaction minima fall at about

$$R = 2.5, 4.4, 6.2, 8.0, 9.8, 11.6\,\text{Å}, \text{etc}\,. \tag{4}$$

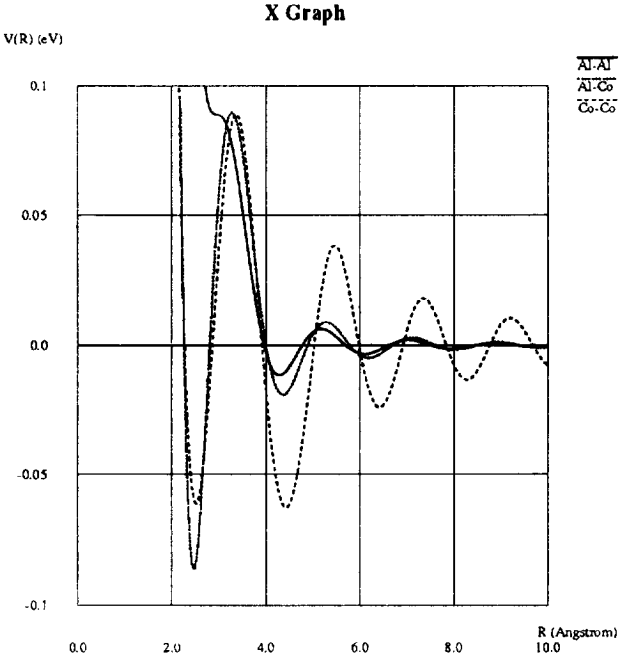

Fig. 1. Pair potentials for Al–Co alloys.

The Al–Al minima occur very near these same separations, except a shoulder, in place of the first minimum, is displaced out to about 2.9 Å. The Co–Co potentials oscillate more strongly than the other two for $R > 4$ Å, and the minima occur at slightly larger separations

$$R = 2.5, 4.4, 6.4, 8.3, 10.1, 11.9 \text{ Å}, \text{etc}. \tag{5}$$

3. Clusters and tilings

The known Al–Co decagonal phase approximants consist of layered structures, alternating flat layers and puckered layers with a 2.0 Å spacing along the pseudo 10-fold axis. Fig. 2 displays parts of a structure known as a "pentagonal bipyramid" (PB), suggested by Henley [4] as a key structural motif in $c = 8$ Å decagonal phases. The aluminum pentagon centered by a cobalt atom forms caps placed at the north and south poles and lies in puckered layers (Fig. 2(a)). The decagonal ring of alternating aluminum and cobalt, centered by an aluminum atom, forms the equator of a pentagonal bipyramid and lies in a flat layer (Fig. 2(b)). The aluminum atoms on the decagonal ring often move inward to the midpoint of a Co–Co bond. The remaining flat layer contains a "junction layer" (not shown here) consisting of a cobalt pentagon and a highly distorted small aluminum pentagon [5].

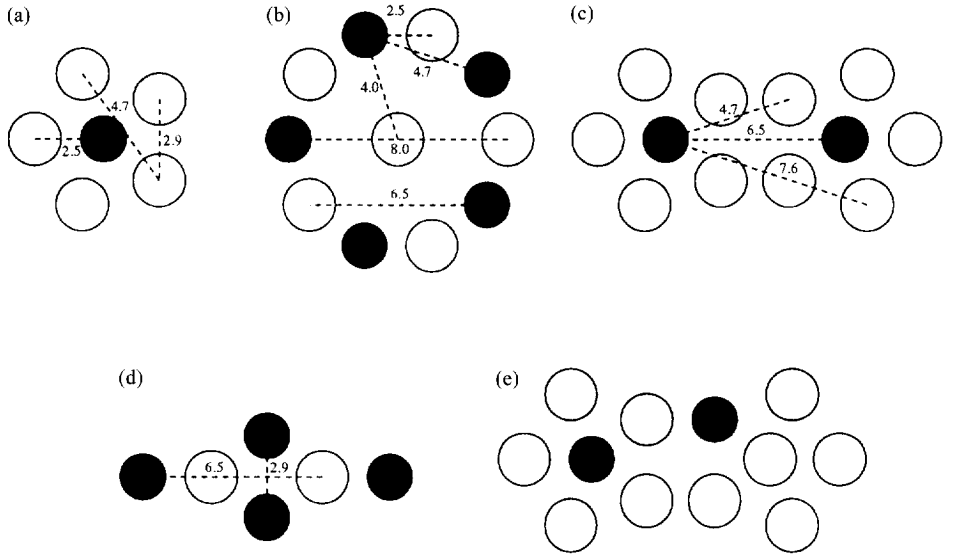

Fig. 2. Pentagonal bipyramid elements: (a) cap lying in puckered layer, (b) equator lying in flat layer, (c) two caps linked by aluminum rectangle, (d) edges of four equators linked by rhombus, (e) characteristic puckered layer defect.

The pentagonal bipyramid exhibits several important interatomic spacings, shown in Fig. 2, that lie close to pair potential minima. The distances shown all lie within atomic layers. Not shown, but equally important, are the following interlayer separations. Close to the second minimum of the Co–Co pair potential are the 4.6 Å spacings between one cap and one equator cobalt, and between two opposite cap cobalts. There are 4.1, 6.2 and 8.6 Å separations between equator cobalts and junction layer cobalts, close to the second, third and fourth minima. Finally, between each cap aluminum and each equator cobalt there are separations of 2.3, 4.4, or 6.4 Å, near, respectively, the first, second and third minima of the Al–Co pair potential.

Interactions *within* the pentagonal bipyramid cluster are thus highly favorable. But interactions *between* these clusters are equally important and favorable. Figs. 2(c) and (d) show favorable linkage between two PB caps (2c) and four PB equators, each attached to one edge of a rhombus (2d). Filling space by linking PBs defines tilings of the puckered and flat layers, with cobalt atoms at tiling vertices. In the puckered layer, the tile edge length is 6.5 Å, and the tiles are stars, boats and hexagons. In the flat layer, the tile edge length is 4.7 Å, and the tiles are pentagons, stars, rhombi and boats. Both of these tiling edge lengths lie near very favorable Co–Co potential minima.

There are many possible such tilings, several of which have been observed in the equilibrium Al–Co phase diagram [6]. Because they are all built out of similar structural elements, linked identically (at near-neighbor level), these phases should be close in free energy. Small changes in composition or temperature should be sufficient to change the stability of one phase with respect to the others.

4. Equilibrium phases

In Figs. 3 and 4 we show radial distribution functions calculated for monoclinic [7] and orthorhombic [8] $Al_{13}Co_4$. These are both decagonal phase approximants with 8 Å periodicity along the pseudo 10-fold axis. They comprise four layers spaced by 2.0 Å along this axis, alternately flat and puckered. Fig. 5 shows monoclinic [9] $Al_{11}Co_4$, which is a 4 Å approximant, comprising one flat and one puckered layer spaced by 2.0 Å along the pseudo 10-fold axis.

Compare the radial distribution function peaks in Fig. 3 with the potentials in Fig. 1. Assuming the composition reported by Hudd and Taylor [7] of $Al_{70.8}Co_{24}$ per unit cell yields an electron density of 0.177 $Å^{-3}$, slightly below pure FCC aluminum. All lengths must be reduced by a factor of 0.992 to reach the electron density of pure FCC aluminum. Prominent peaks in each of the partial distribution functions coincide with minima of the corresponding potential, and the separations noted in our discussion of the pentagonal bipyramid. The only peak at an unfavorable position occurs between Co–Co pairs separated by about 7.6 Å. This peak may be attributed to "second neighbor"

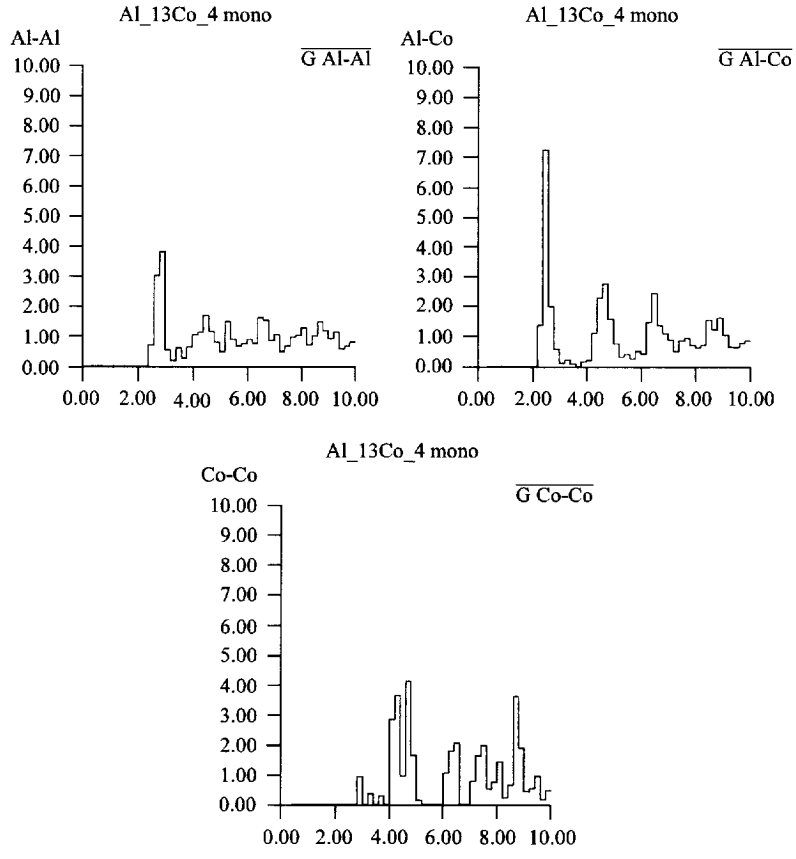

Fig. 3. Radial distribution functions for monoclinic $Al_{13}Co_4$: (a) Al–Al, (b) Al–Co, (c) Co–Co.

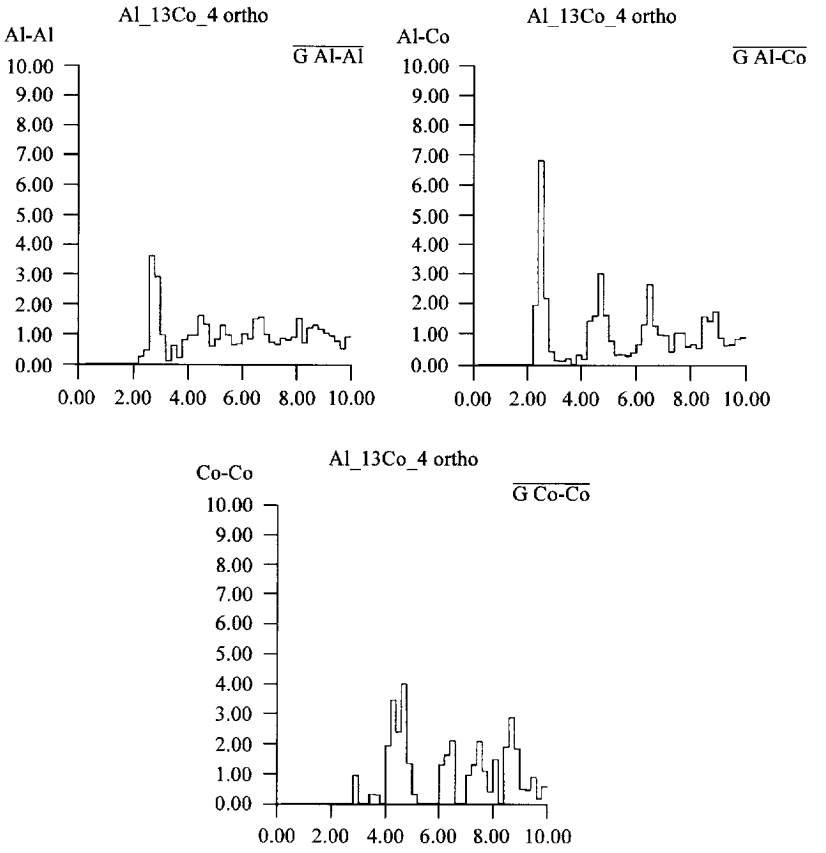

Fig. 4. Radial distribution functions for orthorhombic $Al_{13}Co_4$: (a) Al–Al, (b) Al–Co, (c) Co–Co.

cobalt spacings, both within the PB equator and between PB poles. It is an unavoidable consequence of the pentagonal structures which are otherwise so strongly favorable. Note that for each unfavorable flat-layer Co–Co 7.6 Å pair, there are *two* favorable PB equator–PB junction 8.6 Å Co–Co pairs, which together gain back approximately the energy cost of the 7.6 Å pair.

A few details in Fig. 3 bear comment. First, note that the Co–Co potentials have a strong minimum at a spacing of 2.5 Å, but there is no corresponding peak in the radial distribution function. This exhibits the effective transition metal "repulsion" in aluminum rich alloys. Inspecting the potentials in Fig. 1 it appears the true repulsion is between aluminums with spacings below 4 Å. The Al–Co interaction near 2.5 Å is far below the *average* of the Al–Al and Co–Co interactions. Distributing the Co so as to replace Al–Al bonds with Al–Co minimizes the total energy. Even so, there are still a few Co–Co pairs present in the flat layers with spacings around 2.9 Å associated with the rhombus illustrated in Fig. 2(d).

A second point of interest are the small and very narrow peaks in the Al–Al and Co–Co radial distribution functions at the layering repeat distance of 8.1 Å. These lie

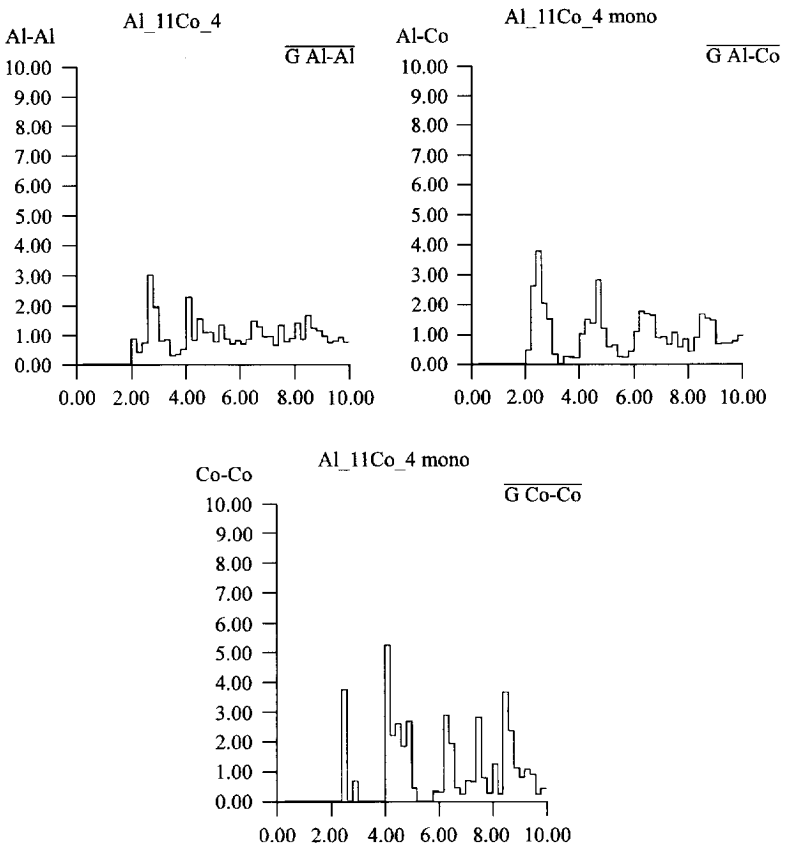

Fig. 5. Radial distribution functions for monoclinic $Al_{11}Co_4$: (a) Al–Al, (b) Al–Co, (c) Co–Co.

fairly close to potential minima, lending stability to structures with this repeat distance. For Co–Co pairs there is another more prominent peak around 8.6 Å, due to the PB equator–PB junction separation discussed above. Both the 8.1 and the 8.6 Å peaks enjoy favorable energies from the potential minimum at 8.3 Å.

Finally, in Fig. 3, note that the Al–Al correlations are weak in magnitude compared with either Co–Co or Al–Co. This suggests that aluminum atoms occupy a wide variety of sites, while cobalt atoms occupy only a small number of distinct types of site. Oscillations of the Al–Co and Co–Co radial distribution functions continue to large distances, with $g_{CoCo}(r)$ oscillating between 0.5 and 1.5 all the way out to $r = 20$ Å.

Fig. 4 displays the radial distribution functions for the orthorhombic variant of $Al_{13}Co_4$ according to the structure determination of Grin et al. [8]. They claim 100% atomic occupancy, yielding an electron density of 0.191 $Å^{-3}$. All distances in Fig. 4 must be increased by the factor 1.018 for comparison with the pair potentials in Fig. 1. Note that the radial distribution function bears striking resemblance to the monoclinic variant. That is no surprise, since they are built out of identical structural elements

assembled in slightly different ways in the two approximants. The similarity of radial distribution functions in turn explains the reported near degeneracy of the two structural energies [1].

The 4 Å approximant, $Al_{11}Co_4$, shown in Fig. 5 shares many correlation features with the previous two structures. The electron density (assuming full occupancy) is $0.193\,Å^{-3}$, so one must increase all lengths by the factor 1.022. One new feature is the presence of a strong Co–Co distribution peak near 2.5 Å. This may arise because $Al_{11}Co_4$ is a high temperature phase [1]. The energy minimizing considerations that disfavor Al–Al (and therefore Co–Co) neighbors could be mitigated by some gain in vibrational or configurational entropy. Indeed, Co–Co separations near 2.5 Å also appear in our high temperature Monte Carlo simulations reported below. These separations enter in our simulation through substitutional disorder of cobalt on certain nominally aluminum sites. This is a component of phason disorder in the selection of cobalt sites.

5. Monte Carlo simulations

In order to model larger approximants to the decagonal phase, which should resemble the decagonal phase even more closely than the smaller approximants do, we define atomic surfaces that give ideal atomic sites by the cut and project method [5]. There is general agreement among several experiments concerning the position and approximate size of atomic surfaces. The details of exact size and shape are not settled by experiment, so we define deliberately oversized atomic surfaces [5]. Then, by Monte Carlo simulation, we allow atoms to populate the favored sites. Relaxation and lattice vibration effects vanish [10] because of our discretization of space. The energy of a configuration in our simulation is its pair potential energy calculated using the pair potentials in Fig. 1.

The simulation generates an ensemble of plausible configurations. Most of them fill space with pentagonal bipyramids, in agreement with suggestions by Henley [4]. During the simulation several distinct tilings occur which suggests that the equilibrium decagonal phase could be a random tiling of PB motifs. Motion of atoms corresponding to "phason jumps" occur frequently, as well as point defects such as vacancies or chemical substitution. A collective series of phason jumps can result in a "tiling flip" converting one PB tiling into another. The sites exhibiting the most frequent occupancy fluctuations are those located near the edges of the atomic surfaces.

Fig. 6 shows the radial distribution functions averaged over a long run at $T = 1000\,K$. An orthorhombic cell $23.4 \times 19.9 \times 16.2\,Å^3$ containing 400 aluminum and 128 cobalt atoms was used. To scale to the FCC aluminum electron density, increase all lengths by the factor 1.015. The energetic and structural similarity between our simulated structures and the known approximants is evident by comparing peaks of the radial distribution functions. Note the presence of Co–Co separations around 2.3–2.7 Å. One important contribution to these distributions comes when a cobalt centering an aluminum pentagon swaps positions with a neighboring aluminum. A new

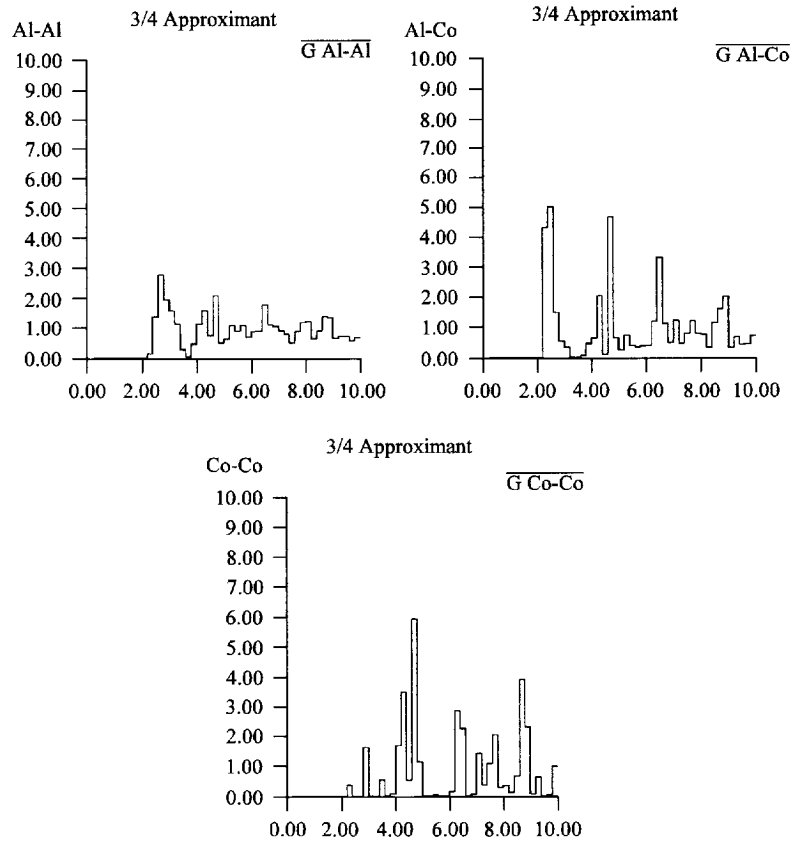

Fig. 6. Radial distribution functions for 3/4 approximant calculated by Monte Carlo simulation at $T = 1000$ K: (a) Al–Al, (b) Al–Co, (c) Co–Co.

cobalt spacing of 4.7 Å appears in the puckered layer (refer to Fig. 2(c) and (e)), reproducing a cobalt spacing characteristic of flat layers. The displaced cobalt lies a distance between 2.3 and 2.7 Å (depending on the direction of its puckering) from a cobalt in the adjacent flat layer. Similar configurations appear in the high temperature monoclinic phase of $Al_{11}Co_4$. Thus the distributions at 4.7 Å and below 2.8 Å are stronger in our simulation than in, for example, the experimental $Al_{13}Co_4$ structure. Our set of allowed "ideal" sites does not include all the sites needed to reach the full experimental 4 Å monoclinic $Al_{11}Co_4$ structure.

6. Conclusions

In summary, we show that several Al–Co decagonal phase approximants, both real and hypothetical, exhibit similarities in their radial distribution functions. Up to 10 Å the distribution peaks match closely the interatomic spacings in a pentagonal bipyramid

(PB) cluster. This atomic cluster, and links between clusters, are strongly favored energetically because interatomic separations occur near pair potential minima. The similarity of the radial distribution functions suggests near degeneracy in total energy of several different structures based upon PB tilings. Significant correlations extend well beyond 10 Å, and are much stronger for Al–Co and Co–Co pairs than for Al–Al pairs.

Acknowledgements

This work was supported in part under NSF grant DMR-9221596.

References

[1] B. Grushko, R. Wittenberg, K. Bickmann and C. Freiburg, Proc. 5th Int. Conf. on Quasicrystals, C. Farot and R. Mosseri, eds. (World Scientific, Singapore, 1995) p. 684.
[2] X.L. Ma and K.H. Kuo, Met. Trans. 23A (1992) 1121.
[3] R. Phillips, J. Zou, A.E. Carlsson and M. Widom, Phys. Rev. B 49 (1994) 9322.
[4] C.L. Henley, J. Non-Cryst. Solids 153–154 (1993) 172; related structural motifs are described in P.J. Black, Acta Crystallogr. 8 (1955) 43; 8 (1955) 175; V. Kumar, D. Sahoo and G. Athithan, Phys. Rev. B 34 (1986) 6924.
[5] E. Cockayne, M. Widom and M. de Graef, Phil. Mag, to be submitted.
[6] X.L. Ma, X.Z. Li and K.H. Kuo, Acta Crystallogr. B51 (1995) 36; X.L. Ma and K.H. Kuo, Phil. Mag. A71 (1995) 687.
[7] R.C. Hudd and W.H. Taylor, Acta Crystallogr. 15 (1962) 441.
[8] J. Grin, U. Burkhardt, M. Ellner and K. Peters, J. Alloys Compounds 206 (1994) 243.
[9] X.Z. Li et al., Phil. Mag. Lett. 72 (1995) 79.
[10] G. Ceder, Comput. Mat. Sci. 1 (1993) 144.
[11] A.P. Tsai, A. Inoue and T. Masumoto, Mat. Trans. JIM 30 (1989) 463.
[12] J.A. Moriarty, Phys. Rev. B 38 (1988) 3199.